Dissipative exciton transfer in donor–bridge–acceptor systems: numerical renormalization group calculation of equilibrium properties



2006 J. Phys.: Condens. Matter 18 5985

(http://iopscience.iop.org/0953-8984/18/26/017)

INSTITUTE OF PHYSICS PUBLISHING JOURNAL OF PHYSICS: CONDENSED MATTER

J. Phys.: Condens. Matter **18** (2006) 5985–6000 doi:10.1088/0953-8984/18/26/017

# Dissipative exciton transfer in donor–bridge–acceptor systems: numerical renormalization group calculation of equilibrium properties

**Sabine Tornow**[1], **Ning-Hua Tong**[2,3] **and Ralf Bulla**[1]

[1] Theoretische Physik III, Elektronische Korrelationen und Magnetismus, Universität Augsburg, 86135 Augsburg, Germany
[2] Institut für Theorie der Kondensierten Materie, Universität Karlsruhe, 76128 Karlsruhe, Germany

Received 13 February 2006
Published 19 June 2006
Online at stacks.iop.org/JPhysCM/18/5985

**Abstract**

We present a detailed model study of exciton transfer processes in donor–bridge–acceptor (DBA) systems. Using a model which includes the intermolecular Coulomb interaction and the coupling to a dissipative environment we calculate the phase diagram, the absorption spectrum as well as dynamic equilibrium properties with the numerical renormalization group. This method is non-perturbative and therefore allows one to cover the full parameter space, especially the case when the intermolecular Coulomb interaction is of the same order as the coupling to the environment and perturbation theory cannot be applied. For DBA systems with up to six sites we found a transition to the localized phase (self-trapping) depending on the coupling to the dissipative environment. We discuss various criteria which favour delocalized exciton transfer.

## 1. Introduction

Exciton transfer belongs to the key processes in many chemical and biological systems, organic based nanostructures and semiconductors [1–3]. The progress in manufacturing molecular electronic devices, biological hybrid systems, and model systems based on quantum dots, nanoscale molecular aggregates and bio-engineered proteins opens the door to understanding these fundamental processes [4] and also to finding applications in (bio-) molecular electronics, biosensing, and quantum computation [5].

Excitons are electron–hole pairs which do not transfer charge but energy, by the deexcitation of a donor molecule followed by the excitation of an acceptor molecule. The radiationless excitation transfer is caused by dipole and exchange interactions and proceeds via a short lived virtual photon [6]. In this work we consider Frenkel excitons [7] where the exciton is a molecular excitation with an electron in the lowest unoccupied molecular orbital

[3] Present address: Department of Physics, Renmin University of China, Beijing 100872, People's Republic of China.

(LUMO) and a hole in the highest occupied molecular orbital (HOMO) on the same molecule. Here the Coulomb coupling of the electron–hole pair is much larger than the hopping matrix element of a single hole or electron. Exciton transfer where the Frenkel exciton concept can be applied occurs in many bio-molecules: e.g., rhodopsin, porphyrins, blue copper protein, carotenoids, and chlorophylls. A well studied molecule is the light-harvesting antenna (LH-II) from the bacterial photosystem *Rhodopseudomonas acidophila*. It is characterized by a symmetric structure and composed of nine identical units forming a ring. Each unit is composed of a chlorophyll dimer. The light-harvesting complexes store and transfer excitations with high efficiency.

In the photosynthetic process an LH-II ring absorbs a photon. The excitation is transferred to other LH-II rings and sent via the LH-I ring to the reaction centre and then converted to chemical energy. The excitation in the LH-II ring B850 can move over the whole ring—it is delocalized over the ring. In other rings, such as B800, the excitations are usually considered to be more localized [4]. Furthermore, mechanisms exist which dissipate excitation energy to save the organism from damage [8]. The degree of delocalization depends strongly on the coupling to the vibronic environment and may be crucial for the function of the specific protein.

The interpretation of optical spectra [9] requires a theory which incorporates both static and dynamic disorder. If the fluctuations of the protein environment occur on a much larger timescale than those of the excitonic system, the disorder is regarded as static. Such a static disorder can be treated by a thermodynamic average. The dynamic disorder stems from the coupling of the electronic degrees of freedom to the fluctuations of the environment. In the present paper we will study the effect of dissipation while neglecting static disorder.

A full *ab initio* quantum chemical calculation of molecules which show exciton transfer reactions is impossible; therefore it is reasonable to investigate the system using simple models which, nevertheless, cover the relevant physics of the problem. The most elementary non-trivial model which describes quantum dissipation is the well studied spin-boson model [10, 11]. It can be viewed as an archetype for modelling the system–environment interaction in bio-molecules in which the electronic degrees of freedom couple to a dissipative environment.

A variety of theoretical methods have been developed to calculate absorption spectra and rates (see, e.g., [12–19]). Some investigations of exciton transfer systems were based on perturbation theory in the exchange coupling between the excitons or in the coupling of the electronic system to the vibrations. If the exciton–vibrational coupling $\alpha$ is weak compared to the dipole–dipole coupling, density-matrix theory is used [3]. If the intermolecular Coulomb coupling $J$ is small we are in the limit of nonadiabatic exciton transfer. Here perturbation theory is applicable, which leads to the Förster equations [3].

A key challenge for a theoretical study of exciton transfer is to cover the whole range of possible behaviour, from coherent to incoherent transfer or even localization or self-trapping of the excitations. Here we use the non-perturbative numerical renormalization group (NRG) to calculate equilibrium properties of the exciton system in the full parameter space. We give a detailed study of the phase diagram, dynamic equilibrium properties for chains and rings up to six sites, and the frequency dependent linear absorption spectra of excitons in a dimer and trimer molecule as a function of the coupling to the bosonic bath. The behaviour of the system is governed by the competition between the couplings $J$ and $\alpha$ which determine whether the excitations are delocalized or localized.

The models we are considering here describe general electron–boson systems with a limited number of quantum states on a few sites with a coupling to a (quantum) dissipative environment. We restrict ourselves to donor, acceptor, and bridge molecules with only two electronic levels per molecule, neglecting the spin degree of freedom. Each site is filled with one spinless electron.

If the flux of photons is sufficiently low then the exciton migration in systems such as a pigment network can be satisfactorily modelled by a single excitation. We show that in the single-exciton subspace the multi-site electron–boson model can be mapped to a multi-site exciton–boson model. The two-site exciton–boson model is identical to the spin-boson model. The exciton system is coupled to all degrees of freedom of the (protein) environment which is modelled by an infinite set of harmonic oscillators. After the discussion of the various models in section 2, we introduce the NRG approach used here in section 3. Section 4 is devoted to the results for the phase diagram, dynamic properties, and the absorption spectrum. We show how the degree of delocalization depends on the different Coulomb interactions, the coupling to the bosonic bath, and the geometric structure.

## 2. Model

In general we describe the problem by a small electronic system like a short chain of molecules with the electronic part $H_{\mathrm{el}}$ coupled via the $H_{\mathrm{el-bath}}$ part to the vibronic degrees of freedom incorporated in $H_{\mathrm{bath}}$:

$$H = H_{\mathrm{el}} + H_{\mathrm{el-bath}} + H_{\mathrm{bath}}. \tag{1}$$

The parameters of the small electronic system can be extracted in principle from quantum chemical calculations [20, 21]. The simplest possible modelling is a two-state system with the two states corresponding to the electron being located at the donor or at the acceptor site. In this case, the electronic part can be modelled via

$$H_{\mathrm{el}} = \sum_{i=A,D} \epsilon_i c_i^\dagger c_i - t(c_A^\dagger c_D + c_D^\dagger c_A), \tag{2}$$

which is equivalent to the spin-boson model. Apparently, models of this kind where the electrons are allowed to hop between donor and acceptor sites (with hopping matrix element $t$) are connected to electron transfer problems. In this paper we do not consider such hopping processes and focus on excitation transfer induced by a two-particle interaction term in the Hamiltonian.

In the current work, we explore excitons in a chain using the Hamiltonian

$$H_{\mathrm{el}} = \sum_{ik=0,1} \epsilon_{ik} c_{ik}^\dagger c_{ik} + \sum_{ij} J_{ij}(c_{i0}^\dagger c_{j1}^\dagger c_{j0} c_{i1} + \mathrm{h.c.}), \tag{3}$$

where each site of the electronic system is represented by two levels (the ground state 0 and the excited state 1). The operators $c_{i0/1}^{(\dagger)}$ denote annihilation (creation) operators for the electrons on site $i$ in the level $0/1$, $\epsilon_{ik}$ is the on-site energy at site $i$ and level $k$ and $J_{ij}$ the exchange interaction between site $i$ and $j$. We neglect the single-electron hopping between neighbouring sites as well as spin degrees of freedom. Therefore, the excitations (Frenkel excitons) can only be transferred via the Coulomb coupling. Similar models were discussed, for example, in [3, 16, 18, 22]. We consider a filling of one spinless electron on each site.

The Hamiltonian equation (3) describes a coherent motion of the excitation through the whole system; this coherence can be destroyed in the presence of a dissipative environment. Here, the coupling to the environment is due to the change of the dipole moment of the molecule during the transition. Simulations showed that the coupling involves essentially all nuclear degrees of freedom of the protein which have to be described quantum mechanically [23]. Even at physiological temperatures there are many degrees of freedom in proteins with frequencies high enough to make a quantum mechanical description necessary. We represent the vibrations of the environment by a set of harmonic oscillators similar to the spin-boson model.

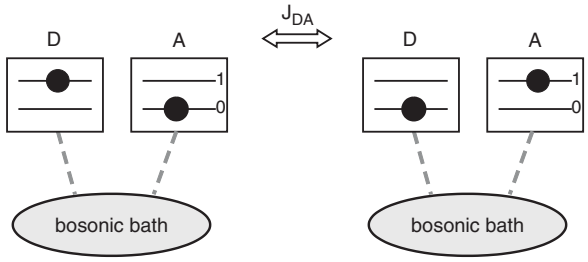


**Figure 1.** Schematic view of the two-site electron–boson model. The transfer integral for the exciton transfer between donor ($D$) and acceptor ($A$) sites is given by $J$. Dissipation in the exciton transfer process is due to the coupling to a common bosonic bath.

The last term in equation (1) describes the free bosonic bath

$$H_{\text{bath}} = \sum_n \omega_n b_n^\dagger b_n, \tag{4}$$

with the bosonic annihilation (creation) operators $b_n^{(\dagger)}$. The second term in equation (1) describes the coupling of the electrons to the bosonic bath

$$H_{\text{el-bath}} = P_{\text{el}} \sum_n \lambda_n \left(b_n^\dagger + b_n\right), \tag{5}$$

where $\lambda_n$ is the coupling strength to the $n$th oscillator. We consider a standard site-diagonal dipole coupling with the polarization operator $P_{\text{el}} = \sum_i g_i n_i$ of the electronic system. The values of the interaction constant $g_i$ of the $i$th site to the bosonic bath will be specified below for the specific number of sites in a chain or ring. The ring is defined as a chain with periodic boundary conditions.

In analogy to the spin-boson model [10, 11], the coupling of the electrons to the bath degrees of freedom is completely specified by the bath spectral function

$$J(\omega) = \pi \sum_n \lambda_n^2 \delta(\omega - \omega_n). \tag{6}$$

Several parameterizations of $J(\omega)$ have been studied in the literature [10]. For a given system, the bath spectral function can also be calculated using molecular dynamics simulations [17]. Here we restrict ourselves to a simple ohmic spectral function and will use more realistic spectral functions in a future study.

### *2.1. Dimer*

For the dimer (that is the two-site electron–boson model as sketched in figure 1) the Hamiltonian equation (1) has the following electronic part:

$$H_{\text{el}} = \sum_{i=D_0,D_1,A_0,A_1} \varepsilon_i c_i^\dagger c_i + J\left(c_{D_0}^\dagger c_{A_1}^\dagger c_{D_1} c_{A_0} + \text{h.c.}\right), \tag{7}$$

and the coupling term

$$P_{\text{el}} = \tfrac{1}{2}(n_{D_1} - n_{D_0} + n_{A_0} - n_{A_1}). \tag{8}$$

The indices $D_0$, $A_0$ indicate the ground state on the donor/acceptor and $D_1$, $A_1$ the first excited states on the donor/acceptor.

We consider one electron on each site so that the electronic degrees of freedom can be represented by the following four-dimensional basis:

$$|i\rangle = \{|0,0\rangle, |1,0\rangle, |0,1\rangle, |1,1\rangle\}, \tag{9}$$

with the notation $|D; A\rangle$ describing the donor/acceptor in the ground state ($D/A = 0$) or in the excited state ($D/A = 1$). Introducing the notation

$$\hat{Y} = \sum_n \omega_n b_n^\dagger b_n, \qquad \hat{X} = \tfrac{1}{2} \sum_n \lambda_n \left( b_n^\dagger + b_n \right), \tag{10}$$

we arrive at the matrix $M = M_0 + M_\mathrm{b} = \langle i | H_\mathrm{dimer} | j \rangle (i, j = 1 \ldots 4)$, where the matrix elements are taken only with respect to the electronic states:

$$M_0 = \begin{pmatrix} \epsilon_{D_0} + \epsilon_{A_0} & 0 & 0 & 0 \\ 0 & \epsilon_{D_1} + \epsilon_{A_0} & J & 0 \\ 0 & J & \epsilon_{D_0} + \epsilon_{A_1} & 0 \\ 0 & 0 & 0 & \epsilon_{D_1} + \epsilon_{A_1} \end{pmatrix}, \tag{11}$$

and

$$M_\mathrm{b} = \begin{pmatrix} \hat{Y} & 0 & 0 & 0 \\ 0 & \hat{Y} - \hat{X} & 0 & 0 \\ 0 & 0 & \hat{Y} + \hat{X} & 0 \\ 0 & 0 & 0 & \hat{Y} \end{pmatrix}. \tag{12}$$

With $\epsilon_{D_0} = \epsilon_{A_0} = 0$ and $\epsilon_{D_1} = \epsilon_D, \epsilon_{A_1} = \epsilon_A$ the eigenvalues of the electronic part $M_0$ are

$$E_1 = 0,$$
$$E_2 = \epsilon_D + \epsilon_A,$$
$$E_{3,4} = \frac{\epsilon_D + \epsilon_A}{2} \pm \sqrt{\frac{(\epsilon_D - \epsilon_A)^2}{4} + J^2}.$$

The eigenstates with energies $E_{3,4}$ are linear combinations of the basis states $|1, 0\rangle$ and $|0, 1\rangle$.

The Hamiltonian of the dimer can be decomposed into subspaces of zero, one, and two excitons. For the subspace with one exciton in the dimer, the basis equation (9) reduces to $|i\rangle = \{|1, 0\rangle, |0, 1\rangle\}$ and the matrix $M$ reads

$$M = \begin{pmatrix} \epsilon_A + \hat{Y} - \hat{X} & J \\ J & \epsilon_D + \hat{Y} + \hat{X} \end{pmatrix}. \tag{13}$$

This matrix allows for an exact mapping onto the spin-boson model (for a similar discussion, see [24]) and the model is equivalent to equation (21) with $N = 2$.

### 2.2. Trimer

The Hamiltonian for a donor–bridge–acceptor system in a trimer geometry (see figure 2) takes the form

$$H_\mathrm{el} = \sum_{i=D_0, D_1, A_0, A_1, B_0, B_1} \varepsilon_i c_i^\dagger c_i + J_{DA} \left( c_{D_0}^\dagger c_{A_1}^\dagger c_{D_1} c_{A_0} + \mathrm{h.c.} \right) + J_{AB} \left( c_{B_0}^\dagger c_{A_1}^\dagger c_{B_1} c_{A_0} + \mathrm{h.c.} \right) + J_{BD} \left( c_{B_0}^\dagger c_{D_1}^\dagger c_{B_1} c_{D_0} + \mathrm{h.c.} \right). \tag{14}$$

The electrons are coupled to the bosonic bath via the polarization operator:

$$P_\mathrm{el} = n_{D_1} - n_{D_0} + n_{A_0} - n_{A_1}. \tag{15}$$

The basis for the electronic degrees of freedom is now composed of eight states (each site is filled with one spinless electron):

$$|1\rangle = |0, 0, 0\rangle, \quad |2\rangle = |1, 1, 1\rangle, \quad |3\rangle = |1, 0, 0\rangle, \quad |4\rangle = |0, 1, 0\rangle,$$
$$|5\rangle = |0, 0, 1\rangle, \quad |6\rangle = |1, 1, 0\rangle, \quad |7\rangle = |0, 1, 1\rangle, \quad |8\rangle = |1, 0, 1\rangle,$$

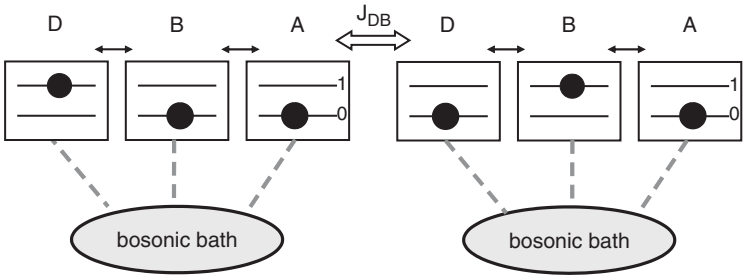


**Figure 2.** Schematic view of the three-site electron–boson model. The Coulomb matrix element of excitons between donor ($D$), bridge ($B$) and acceptor ($A$) sites is given by $J$. Dissipation in the exciton transfer process is due to the coupling of the electronic degrees of freedom to a common bosonic bath. The excitation transfer shown in the figure is due to the coupling $J_{DB}$. We also consider periodic boundary conditions (ring) with a finite matrix elements $J_{DA}$.

where the 0(1) indicates an occupied first (second) level, respectively, with the notation $|D, B, A\rangle$ for the occupation of donor, bridge, and acceptor molecule. A direct hopping of the exciton is possible from the donor to the acceptor or to the bridge and from the acceptor to the bridge and back. The matrix elements now read:

$$\begin{aligned}
\langle 1|H|1\rangle &= \epsilon_{D_0} + \epsilon_{B_0} + \epsilon_{A_0} + \hat{Y} + \left(g_{B_0} + g_{D_0} + g_{A_0}\right)\hat{X},\\
\langle 2|H|2\rangle &= \epsilon_{D_1} + \epsilon_{A_1} + \epsilon_{B_1} + \hat{Y} + \left(g_{A1} + g_{D1} + g_{B1}\right)\hat{X},\\
\langle 3|H|3\rangle &= \epsilon_{A_0} + \epsilon_{B_0} + \epsilon_{D_1} + \hat{Y} + \left(g_{A_0} + g_{B_0} + g_{D_1}\right)\hat{X},\\
\langle 4|H|4\rangle &= \epsilon_{D_0} + \epsilon_{B_1} + \epsilon_{A_0} + \hat{Y} + \left(g_{B_1} + g_{D_0} + g_{A_0}\right)\hat{X},\\
\langle 5|H|5\rangle &= \epsilon_{D_0} + \epsilon_{A_1} + \epsilon_{B_0} + \hat{Y} + \left(g_{D_0} + g_{A_1} + g_{B_0}\right)\hat{X},\\
\langle 6|H|6\rangle &= \epsilon_{A_0} + \epsilon_{B_1} + \epsilon_{D_1} + \hat{Y} + \left(g_{B_1} + g_{A_0} + g_{D_1}\right)\hat{X},\\
\langle 7|H|7\rangle &= \epsilon_{D_0} + \epsilon_{B_1} + \epsilon_{A_1} + \hat{Y} + \left(g_{B_1} + g_{D_0} + g_{A_1}\right)\hat{X},\\
\langle 8|H|8\rangle &= \epsilon_{D_1} + \epsilon_{B_0} + \epsilon_{A_1} + \hat{Y} + \left(g_{B_0} + g_{D_1} + g_{A_1}\right)\hat{X},\\
\langle 4|H|5\rangle &= \langle 5|H|4\rangle = J_{AB},\\
\langle 6|H|8\rangle &= \langle 8|H|6\rangle = J_{AB},\\
\langle 3|H|4\rangle &= \langle 4|H|3\rangle = J_{BD},\\
\langle 7|H|8\rangle &= \langle 8|H|7\rangle = J_{BD},\\
\langle 3|H|5\rangle &= \langle 5|H|3\rangle = J_{AD},\\
\langle 6|H|7\rangle &= \langle 7|H|6\rangle = J_{AD}.
\end{aligned} \tag{16}$$

For $\epsilon_{A_1} = \epsilon_{B_1} = \epsilon_{D_1} = \epsilon$ and $J_{AB} = J_{BD} = J_{AD} = J$ the eigenvalues are given by

$$\begin{aligned}
E_1 &= 0,\\
E_2 &= 3\epsilon,\\
E_{3,4} &= \epsilon - J,\\
E_5 &= \epsilon + 2J,\\
E_{6,7} &= 2\epsilon - J,\\
E_8 &= 2\epsilon + 2J.
\end{aligned}$$

For the chain as in figure 2, we set $J_{AD} = 0$ and $J_{AB} = J_{BD} = J$. The resulting (non-degenerate) eigenvalues are

$$E_1 = 0,$$
$$E_2 = 3\epsilon,$$
$$E_3 = 2\epsilon,$$
$$E_4 = \epsilon,$$
$$E_{5,6} = \epsilon \pm \sqrt{2}J,$$
$$E_{6,7} = 2\epsilon \pm \sqrt{2}J.$$

In the subspace with only one exciton, the basis consists of the three states $|1, 0, 0\rangle$, $|0, 1, 0\rangle$, and $|0, 0, 1\rangle$, and the matrix reduces to

$$M = \begin{pmatrix} \epsilon_D + \hat{Y} + 2\hat{X} & J_{AB} & J_{AD} \\ J_{AB} & \epsilon_B + \hat{Y} & J_{BD} \\ J_{AD} & J_{BD} & \epsilon_A + \hat{Y} - 2\hat{X} \end{pmatrix}. \tag{17}$$

The eigenvalues for the trimer with periodic boundary conditions ($J_{AD} \neq 0$) and with $\epsilon_A = \epsilon_B = \epsilon_D = \epsilon$ are

$$E_{1,2} = \epsilon - J,$$
$$E_3 = \epsilon + 2J,$$

and for the chain as in figure 2 the non-degenerate eigenvalues are

$$E_1 = \epsilon,$$
$$E_{2,3} = \epsilon \pm \sqrt{2}J.$$

The model is equivalent to equation (21) with $N = 3$.

For the chain with different couplings of the donor and acceptor to the bridge $J_{AB} \neq J_{DB}$ ($J_{AD} = 0$) the eigenvalues are

$$E_1 = \epsilon,$$
$$E_{2,3} = \epsilon \pm \sqrt{J_{AB}^2 + J_{DB}^2}.$$

The occupancy on the donor and acceptor ($n_D$ and $n_A$) for zero coupling to the bosonic bath at $T = 0$ are

$$\langle n_A \rangle = \frac{1}{2} \frac{J_{AB}^2}{J_{AB}^2 + J_{DB}^2},$$
$$\langle n_D \rangle = \frac{1}{2} \frac{J_{DB}^2}{J_{AB}^2 + J_{DB}^2}. \tag{18}$$

The degeneracy on $D$ and $A$ is lifted for $J_{AB} \neq J_{DB}$. As will be shown below, no phase transition occurs in this case.

### *2.3. Multi-site exciton–boson model*

In the single-exciton subspace, the fermionic degrees of freedom of the models introduced above can be mapped onto operators $a_i^{(\dagger)}$ for a hard-core boson corresponding to the creation and annihilation of an exciton at site $i$. This results in general multi-site exciton–boson models with $N$ sites defined by

$$H_{\text{multi}} = H_{\text{x}} + H_{\text{x-bath}} + H_{\text{bath}}, \tag{19}$$

with the electronic part defined as

$$H_{\mathrm{x}} = \sum_{i,j}^{N} J_{ij} a_i^{\dagger} a_j. \tag{20}$$

The parameters $J_{ij}$ for $i \neq j$ are the transfer integrals between site $i$ and $j$. As before, we only consider nearest neighbour interactions. The diagonal elements $J_{ii}$ are the on-site energies $\varepsilon_i$ at site $i$. We perform a constant shift of the Hamiltonian by $J_{ii} = J_{jj} (\forall i, j)$ and arrive at

$$H_{\mathrm{x}} = \sum_{i,j,i\neq j}^{N} J_{ij} a_i^{\dagger} a_j. \tag{21}$$

For the coupling term we assume the following form:

$$H_{\mathrm{x-bath}} = P_{\mathrm{el}} \sum_{n} \lambda_n \left( b_n^{\dagger} + b_n \right), \tag{22}$$

with the polarization operator $P_{\mathrm{el}}$

$$P_{\mathrm{el}} = \sum_{i}^{N} g_i a_i^{\dagger} a_i = \sum_{i}^{N} (i - (N+1)/2) a_i^{\dagger} a_i. \tag{23}$$

For $N = 2$ the model is equivalent to the spin-boson model with the matrix $M$ as in equation (13), and for $N = 3$ it is equivalent to equation (17).

## 3. Method

The models we are considering here are completely specified by the parameters of the electronic system and the spectral function $J(\omega)$ (defined in equation (6)) which can be estimated in a classical molecular dynamics simulation. We are using here an ohmic form:

$$J(\omega) = 2\pi\alpha\omega\Theta(\omega - \omega_{\mathrm{c}}), \tag{24}$$

where $\alpha$ is the dimensionless coupling for which we use values in the range 0.01–2. The parameter $J$ is measured in units of $\omega_{\mathrm{c}}$. Typical values of $\hbar\omega_{\mathrm{c}}$ are of the order of 1–10 meV.

As described in the introduction, basically all degrees of freedom of the bosonic bath (the dissipative environment) are relevant for the behaviour of the electronic or excitonic system. So it is not possible to disregard high energy states even if we are interested in low temperature properties like the coherent behaviour for temperatures smaller than the characteristic temperature $T^*$. The renormalization group ansatz is designed for problems where every energy scale contributes and perturbation theory typically shows logarithmic divergences at small frequencies (energies) when the temperature goes to zero.

In order to keep the paper self-contained, we explain the numerical renormalization group (NRG) method for the bosonic bath in detail.

Originally the NRG was invented by Wilson for a fermionic bath to solve the Kondo problem [25, 26]. The fermionic NRG is a standard and powerful tool to investigate complex impurity problems with one or more fermionic baths. Only recently was the method extended to treat quantum impurity systems with a coupling to a *bosonic* bath [27, 28]. Here we focus on equilibrium quantities (recently it was shown that the NRG can also be applied to non-equilibrium situations [29, 30].)

For the numerical renormalization procedure we start from the Hamiltonian written in a continuous form (see the detailed discussion in [28]):

$$H = H_{\mathrm{el}} + \int_0^1 \mathrm{d}\varepsilon\, g(\varepsilon) b_{\varepsilon}^{\dagger} b_{\varepsilon} + P_{\mathrm{el}} \int_0^1 \mathrm{d}\varepsilon\, h(\varepsilon) (b_{\varepsilon}^{\dagger} + b_{\varepsilon}). \tag{25}$$

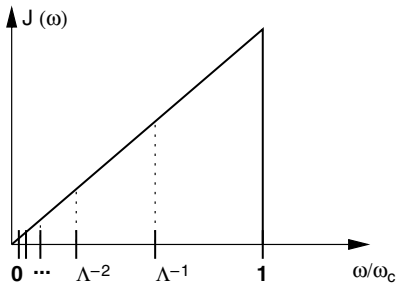


**Figure 3.** Logarithmic discretization of the spectral function $J(\omega)$.

The function $g(\varepsilon)$ is the dispersion of the bosonic bath and $h(\varepsilon)$ characterizes the coupling between the electronic system and the bath. The variable $\varepsilon(x)$ has values from 0 to 1, while $x$ ranges from 0 to $\omega_c$. Both functions are related to the spectral function $J(x) = \pi(\mathrm{d}\varepsilon(x)/\mathrm{d}x)h^2[\varepsilon(x)]$, and $\varepsilon$ is defined as the inverse function of $g$ via $g[\varepsilon(x)] = x$ (see [28]).

We start defining the renormalization group transformations by a logarithmic discretization of the bath spectral function (figure 3) in intervals $[\Lambda^{-n+1}, \Lambda^{-n}]$, with $n = 0, 1, \ldots, \infty$ and $\Lambda > 1$ the NRG discretization parameter. The discretization is exact for $\Lambda \to 1$ and still works very well for $\Lambda = 3$. (Here we are using $\Lambda = 2$.)

Within each of these intervals only one bosonic degree of freedom is retained as a representative of the continuous set of degrees of freedom. The function $h(\varepsilon)$ is chosen to be a constant in each interval of the logarithmic discretization. The Hamiltonian is written in the new discrete basis and the resulting Hamiltonian is mapped onto a semi-infinite chain (figure 4) with the electronic part $H_{\mathrm{el}}$ coupling to the first site of the bosonic chain. Finally the chain-Hamiltonian is numerically diagonalized via successively adding one site to the chain. The effective Hamiltonian is treated on successive smaller energy scales by the renormalization group transformation

$$H_{N+1} = \Lambda H_N + \Lambda^{N+1}\left[\varepsilon_{N+1} b_{N+1}^{\dagger} b_{N+1} + t_N\left(b_N^{\dagger} b_{N+1} + \mathrm{h.c.}\right)\right]. \tag{26}$$

The energies $\varepsilon_n$ and couplings between the elements of the chain $t_n$ are falling off as $\Lambda^{-n}$.

The bosonic NRG has been shown to give very accurate results for the spin-boson model [27, 28]. One of its strengths is the flexibility to handle a variety of models involving the coupling of a small subsystem to a bosonic bath.

There are a few technical steps to perform the iterative diagonalization. To keep the computation time growing only linearly with the number of sites of the semi-infinite chain we are using a truncation scheme where only $N_s \sim 100$ states are retained after each iteration. In addition, we are using a finite number of bosonic basis states $N_b$ for each added site which is of the order 6–10.

To detect possible phase transitions, we calculate the eigenvalue spectrum and the density–density correlation function (see below). In the limit of $\alpha = 0$ the exciton system and the bosonic degrees of freedom are completely decoupled. The coherent motion of the exciton is undamped and we are in the delocalized phase. In contrast, in the case of $J = 0$ the system is in the localized phase. The two phases (localized and delocalized) are connected by a quantum phase transition. Similar to the analysis in [28], the phase diagrams of the exciton–boson models studied here can be obtained from the flow diagram of the lowest-lying many-particle levels. Another possibility is to calculate the density–density autocorrelation function $C(\omega)$ which shows a divergency at the phase transition.

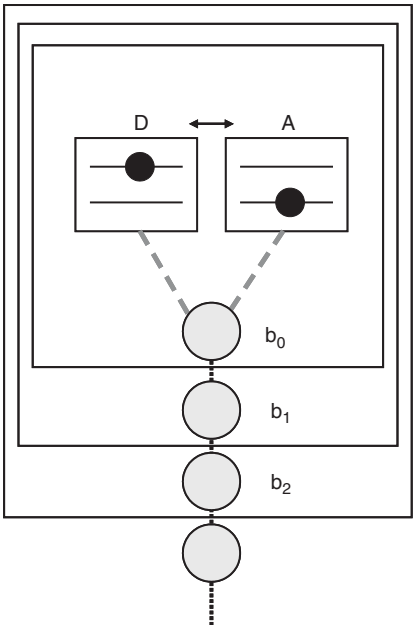


**Figure 4.** Scheme of the bosonic chain-NRG. The boxes represent the iterative diagonalization.

We calculate $C(\omega)$ for the dimer and trimer for different sets of parameters. This quantity is defined by

$$C(\omega) = \frac{1}{4\pi}\int_{-\infty}^{\infty} \mathrm{d}t \mathrm{e}^{\mathrm{i}\omega t}\left\langle [P_{\mathrm{el}}(t),\, P_{\mathrm{el}}(0)]_{+}\right\rangle,$$

and probes the dynamics under equilibrium preparation. For the two-site model, $C(\omega)$ corresponds to the spin–spin correlation function of the equivalent spin-boson model:

$$C(\omega) = \frac{1}{4\pi}\int_{-\infty}^{\infty} \mathrm{d}t \mathrm{e}^{\mathrm{i}\omega t}\left\langle \left[\sigma_z(t), \sigma_z(0)\right]_{+}\right\rangle,$$

with $\sigma_z$ the $z$-component of the spin in this model.

We calculate the density–density correlation function as the sum of $\delta$-functions in the Lehmann representation:

$$C(\omega) = \tfrac{1}{2}\sum_{n} |\langle 0\,|P_{\mathrm{el}}|\,n\rangle|^2\,\delta\left(\omega + \epsilon_0 - \epsilon_n\right), \qquad \omega > 0.$$

The function is symmetric ($C(\omega) = C(-\omega)$).

The linear absorption and emission coefficient $\alpha(\omega)$ for the donor site of the electronic system coupled to the bosonic bath under the influence of an external laser field of frequency $\omega$ is given by Fermi's golden rule:

$$\alpha^{D}(\omega) = 2\pi \sum_{f} \left|\left\langle f \left| H^{D}_{\mathrm{pert}} \right| 0\right\rangle\right|^2 \delta\left(\omega + E_0 - E_f\right), \tag{27}$$

where $H^{D}_{\mathrm{pert}}$ is defined as

$$H^{D}_{\mathrm{pert}} = c^{\dagger}_{D1}c_{D0} + c^{\dagger}_{D0}c_{D1}. \tag{28}$$

The term $H^{D}_{\mathrm{pert}}$ describes the excitation of an electron from the ground state $D_0$ to the excited

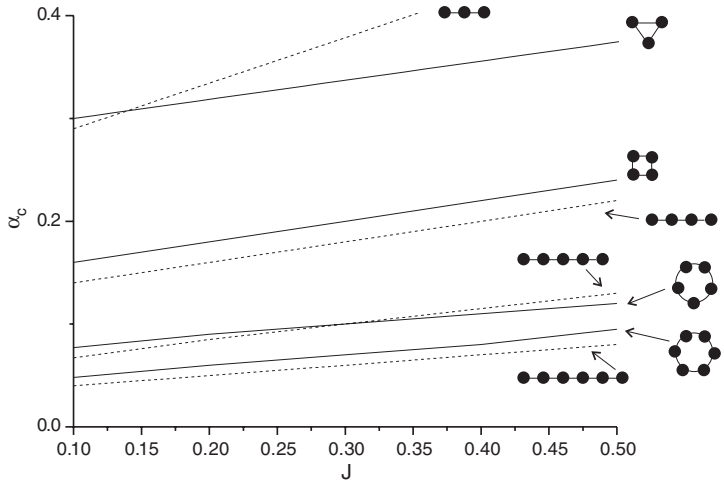


**Figure 5.** Phase diagram of rings (solid line) and chains (dotted line) with 3, 4, 5 and 6 sites. The system is in the localized (delocalized) phase above (below) the phase boundary. The NRG parameters are $N_s = 100$, $N_b = 8$, and $\Lambda = 2$.

state $D_1$. It can be treated perturbatively as long as the probing photon energy is small. For the initial state we use the ground state $|0\rangle$, and $|f\rangle$ are all possible final states.

The eigenenergies of $H$ ($E_0$ and $E_f$) and the matrix elements $\langle 0|H_{\rm pert}|f\rangle$ are evaluated with the NRG for different $J$ and increasing coupling to the bosonic bath. To obtain a continuous curve for $\alpha^D(\omega)$, the $\delta$-functions appearing in equation (27) have to be broadened. Here we use the strategy discussed in [31], that is replacing each $\delta$-function by a Gaussian on a logarithmic scale. On a linear scale, this function is not symmetric around its centre, so the spectral weight in $\alpha^D(\omega)$ appears to be shifted to higher frequencies.

## 4. Results

### *4.1. Phase diagram*

Increasing $J$ tends to delocalize the exciton. Since we have excluded the single-electron hopping in the Hamiltonian, the dynamics can be restricted to the single-exciton subspace which maps onto a spin-boson model for two sites. For increasing coupling to the bosonic bath, the exciton localizes at a critical $\alpha_c$. We explore the phase diagram with localized and delocalized phases (connected by a Kosterlitz–Thouless transition) for the exciton–boson model with 2–6 molecular sites by calculating the critical $\alpha_c(J)$ as a function of $J$. Note that a phase transition occurs only under certain conditions—necessary is the degeneracy in energy and occupancy of at least two sites 1 and 2 (not necessarily neighbours) with the same absolute value of the coupling to the bosonic bath. This degeneracy is lifted if site 1 and 2 have different occupancies, which is the case if the on-site energies of these sites are different, or in larger systems if certain hopping matrix elements have different values. In the absence of a phase transition we see a crossover from a delocalized to a more localized regime.

The phase diagram for the spin-boson model was calculated already in [28]. The critical $\alpha$ depends linearly on the matrix element $J$. It was noted that the exact value of $\alpha_c$ has to be determined in the limit of $\Lambda \to 1$. We do not perform the extrapolation, so the critical $\alpha_c$ is somewhat larger than the actual value.

In figure 5 we display the phase diagram of the multi-site exciton–boson model for 3, 4, 5 and 6 sites for both chain and ring geometry (chain with periodic boundary conditions).

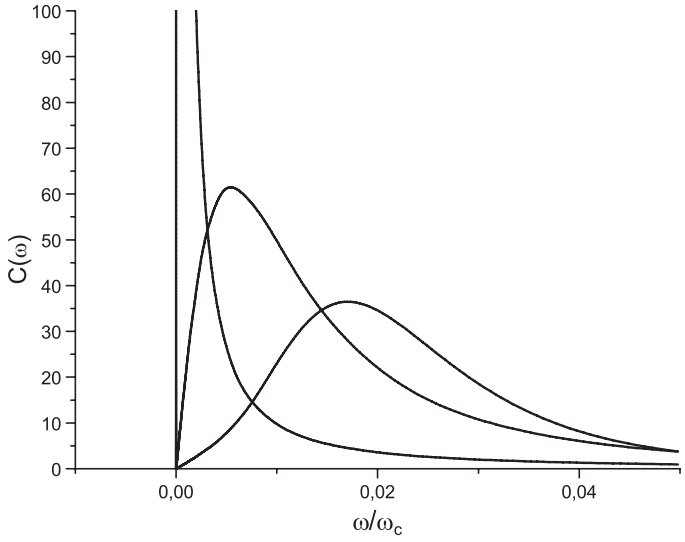


**Figure 6.** Density–density correlation function $C(\omega)$ for the dimer for different $\alpha$ and $J = 0.4$. For small frequencies, $C(\omega)$ is linear in $\omega$. The slope increases with increasing $\alpha = 0.1, 0.2, 0.3$. For zero bias ($\varepsilon = 0$) the phase transition to the localized phase is indicated by an infinite slope. The NRG parameters are $N_s = 100$, $N_b = 8$, and $\Lambda = 2$ here and for all following figures.

The dashed and solid lines display the critical $\alpha_c$ for the chain and ring, respectively. The critical coupling shows a linear behaviour similar to that in the spin-boson model. For an even number of sites the ring has a larger critical $\alpha$ than the chain. For an odd number of sites, both curves cross at a certain value of $J$. Above this $J$ turning off the periodic boundary conditions will tend to delocalize the exciton. This behaviour is probably related to the change of the occupancies on each site. We plan to investigate the intriguing even–odd difference with non-equilibrium methods [29, 30].

For a three-site exciton–boson model no quantum phase transition is observed as soon as the couplings between the donor and bridge $J_{DB}$ as well as acceptor and bridge $J_{AB}$ are different. This lifts the degeneracy in the occupancy on $D$ and $A$. To study the crossover from the delocalized to a more localized phase, we calculate the equilibrium dynamical properties as discussed in the following.

### *4.2. Equilibrium dynamical properties*

To study the dynamics of the electron transfer process in the one-exciton subspace we calculate the density–density correlation function $C(\omega) = \frac{1}{2\pi}\int_{-\infty}^{+\infty} e^{i\omega t} C(t)\, dt$ with

$$C(t) \sim \left\langle [a_D^\dagger a_D(t) - a_A^\dagger a_A(t), a_D^\dagger a_D(0) - a_A^\dagger a_A(0)]_+ \right\rangle, \tag{29}$$

for the dimer ($g_D = 1/2$, $g_A = -1/2$) and for the trimer ($g_B = 0$, $g_A = -1$, $g_D = 1$).

In the two-site case, the density–density correlation function is identical to the spin–spin correlation function. The correlation function shows a power-law behaviour for low frequencies up to $\omega \approx T^*$. When $\alpha$ approaches $\alpha_c$, the slope in $C(\omega)$ increases and the peak position which defines the temperature scale $T^*$ is shifted to lower energies; see figure 6. At the phase transition the correlation function is diverging. The correlation function shows an algebraic long time behaviour for $T = 0$ and an exponential decay for finite $T$.

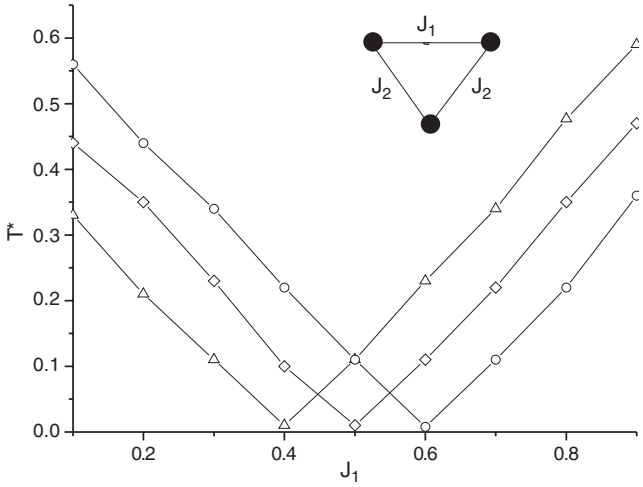


**Figure 7.** Crossover temperature for a trimer ring with $J_2 = J_{AB} = J_{DA} = 0.4$ (triangles), 0.5 (diamonds), 0.6 (circles) and various values of $J_1$. The coupling $\alpha$ is set to 0.1.

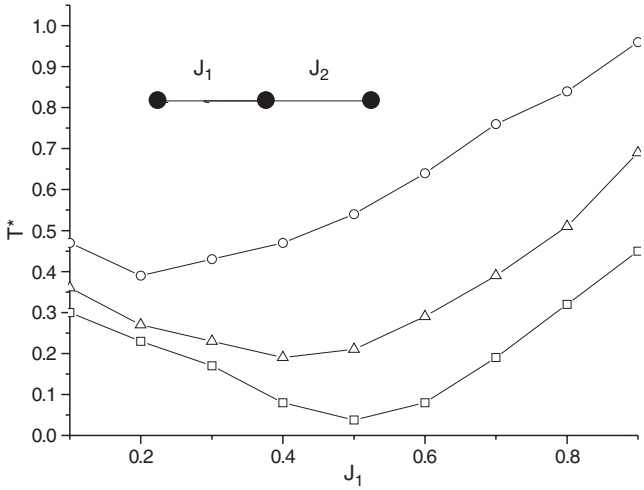


**Figure 8.** Crossover temperature for a trimer chain with $J_2 = 0.5$ and various values of $J_1$. The coupling $\alpha$ is set to 0.1, 0.2 and 0.3 for the upper, middle and lower curve, respectively.

In figure 7 we show results for the characteristic temperature for a trimer ring by keeping $J_{AB} = J_{AD}$ constant and varying $J_1 = J_{DB}$. The value of $T^*$ goes through a minimum at $J_1 = J_{AB} = J_{AD}$. The larger the difference the larger is the characteristic temperature.

In figure 8 we display the characteristic temperature for an asymmetric three-site chain with $J_1 \neq J_2$ for increasing $\alpha$. For large $\alpha$ and $J_1 = J_2$ the characteristic temperature $T^*$ goes to zero indicating the phase transition. For the asymmetric chain no phase transition occurs and $T^*$ increases with the increasing difference of the matrix elements $J_1$ and $J_2$ for $J_1 > J_2$.

### *4.3. Absorption spectrum*

For $\alpha = 0$, the spectrum of the two-site electron–boson model consists of four states. In the ground state, both electrons occupy the lowest level of donor and acceptor molecules,

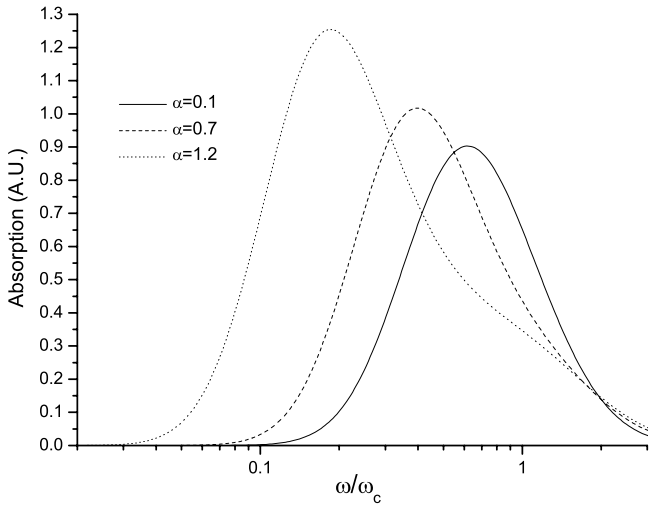


**Figure 9.** Dimer absorption spectrum for $J = 0.2$, $\epsilon_D = \epsilon_A = 0.75\omega_c$ and $\alpha = 0.1, 0.7, 1.2$ as a function of $\omega$.

respectively. The system can be excited by a photon: $D + A \rightsquigarrow D^* + A$. If we now consider a finite $J$, the exciton is able to move to the acceptor and back ($D^* + A \leftrightarrows D + A^*$).

To calculate the absorption spectrum we choose the initial state to be the ground state. The ground state is calculated with the NRG and depends on $\alpha$ and $J$. We set the energy difference between the ground state and the excited state to $\varepsilon = 0.75\omega_c$. For $\alpha = 0$ and $J = 0$, the peak in the absorption spectrum is at $\omega = \varepsilon = 0.75$. For increasing $J$, the peaks are at frequencies equal to the eigenenergies $\omega = \varepsilon \pm J$. If now $\alpha$ is increased the two main peaks are broadened and shifted (see figure 9). The height of the peak at low frequencies increases with increasing $\alpha$.

The absorption spectrum for the trimer with $\alpha = 0$ shows peaks at $\varepsilon + 2J$ and $\varepsilon - J$ for the ring geometry (with $J_{AB} = J_{AD} = J_{BD} = J$) and at $\varepsilon \pm \sqrt{2}J$ for the chain. The absorption spectra for various values of $\alpha$ are shown in figures 10 and 11 for the ring and chain, respectively.

## 5. Conclusion

In this paper we studied the phase diagram, equilibrium dynamical properties and the linear absorption spectrum of Frenkel excitons in models with different sites (with or without periodic boundary conditions) where the electronic degrees of freedom are coupled to a bosonic bath. We used the numerical renormalization group method which allows one to study the electron–boson and exciton–boson models in the full parameter regime.

We studied in detail the phase diagrams of the multi-site electron–boson models in the subspace of one exciton. In the zero-bias case (all molecules have degenerate HOMO and LUMO energies), increasing the value of $\alpha$ leads to a quantum phase transition between a delocalized and a localized phase. For the two-site case (dimer) the exciton–boson model can be mapped onto the spin-boson model for which the phase diagram is already known. For more than two sites, the behaviour is more complicated and depends also on the boundary conditions (chain versus ring).

The calculation of the density–density correlation function allows one to estimate the characteristic temperature for the crossover between delocalized and localized phase. This

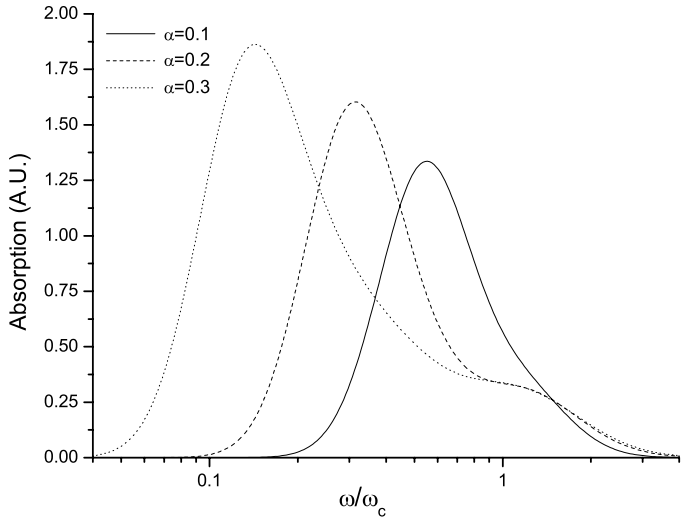


**Figure 10.** Absorption spectrum of a trimer ring for $J = 0.2$, $\epsilon_D = \epsilon_A = 0.75\omega_c$ and $\alpha = 0.1, 0.2, 0.3$ as a function of $\omega$. The NRG parameters are $N_s = 100$, $N_b = 8$ and $\Lambda = 2$.

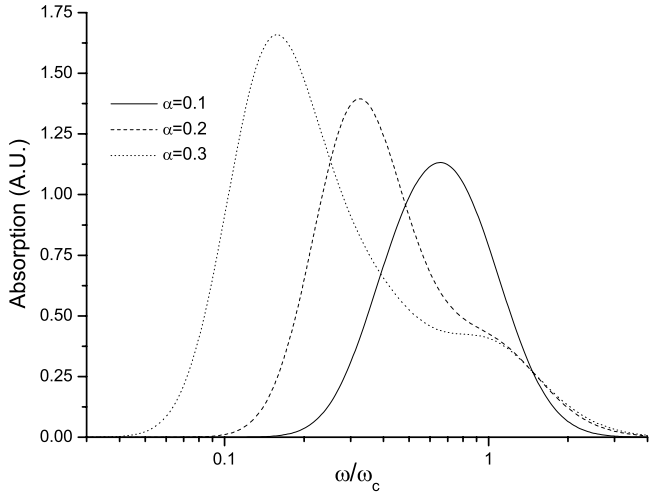


**Figure 11.** Chain absorption spectrum for $J = 0.3$, $\epsilon_D = \epsilon_A = 0.75\omega_c$ and $\alpha = 0.1, 0.2, 0.3$.

crossover temperature $T^*$ is zero for the localized phase and increases when the system goes to the delocalized phase.

In the trimer we investigated different coupling between the donor and bridge as well as the acceptor and bridge. The degeneracy of the occupation on acceptor and donor is lifted, which leads to the disappearance of a phase transition (similar to the change of the on-site energies). Changing the coupling between donor and bridge ($J_{DB}$) with fixed coupling between acceptor and bridge ($J_{AB}$) leads generally to a more delocalized behaviour for $J_{DB} > J_{AB}$.

It would be interesting to compare our results to optical experiments of small bio-engineered systems or quantum dots in which exciton transfer occurs. Further studies are planned to evaluate the time dependent behaviour of excitons, to extend the system to larger

rings and to include static disorder using time dependent and equilibrium NRG to model systems like the LH-II ring.

## Acknowledgments

We acknowledge helpful discussions with U Kleinekathöfer, M Wubs, and D Vollhardt. This research was supported by the DFG through SFB 484 (ST, RB), the Center for Functional Nanostructures (NT), and by the Alexander von Humboldt foundation (NT).

## References

[1] Hu X, Ritz T, Damjanovic A, Autenrieth F and Schulten K 2002 *Q. Rev. Biophys.* **35** 1–62
[2] Agranovich V M and Bassani G F 2003 Thin films and nanostructures *Electronic Excitations in Organic Based Nanostructures* vol 31 (Amsterdam: Elsevier)
[3] May V and Kühn O 2004 *Charge and Energy Transfer Dynamics in Molecular Systems* (Weinheim: Wiley)
[4] Fleming G R and Scholes G D 2004 *Nature* **431** 256
[5] Nazir A, Lovett B W and Briggs G A D 2004 *Phys. Rev.* A **70** 052301
[6] Danjanovic A, Ritz T and Schulten K 1999 *Phys. Rev.* E **59** 3293
[7] Davydov A S 1962 *Theory of Molecular Excitons* (New York: McGraw-Hill)
[8] Jordanides X J, Scholes G D, Shapley W A, Reimers J R and Fleming G R 2004 *J. Phys. Chem.* B **108** 1753
[9] Mukamel S 1995 *Principles of Nonlinear Optical Spectroscopy* (New York: Oxford University Press)
[10] Leggett A J, Chakravarty S, Dorsey A T, Fisher M P A, Garg A and Zwerger W 1987 *Rev. Mod. Phys.* **59** 1
[11] Weiss U 1999 *Quantum Dissipative Systems* 2nd edn (Singapore: World Scientific)
[12] Haken H and Reineker P 1972 *Z. Phys.* **249** 253
Haken H and Strobl S 1973 *Z. Phys.* **262** 135
[13] Agranovich V M and Galanin M D 1982 *Electronic Excitation Energy Transfer in Condensed Matter* (Amsterdam: Elsevier)
[14] Cheng Y C and Silbey R J 2006 *Phys. Rev. Lett.* **96** 028103
[15] Wubs M and Knoester J 1998 *Chem. Phys. Lett.* **284** 63
[16] Herman P and Barvik I 2001 *Chem. Phys.* **274** 199
[17] Kleinekathöfer U, Schröder M and Schreiber M 2005 *J. Lumin.* **112** 461
[18] Damjanovich A, Kosztin I, Kleinekathöfer U and Schulten K 2002 *Phys. Rev.* E **65** 031919
[19] Redfield A G 1965 *Adv. Magn. Reson.* **1** 1
[20] Di Felice R A, Calzolari A, Varsano D and Rubio Secades A 2006 *Introducing Molecular Electronics* ed G Cuniberti, K Richter and G Fargas (Heidelberg: Springer)
[21] Starikov E B 2003 *Phil. Mag. Lett.* **83** 699
[22] Gilmore J and McKenzie R H 2005 *J. Phys.: Condens. Matter* **17** 1735
[23] Xu D and Schulten K 1994 *Chem. Phys.* **182** 91
[24] Tornow S, Tong N H and Bulla R 2006 *Eur. Phys. Lett.* **73** 913
[25] Wilson K G 1975 *Rev. Mod. Phys.* **47** 773
[26] Krishna-murthy H R, Wilkins J W and Wilson K G 1980 *Phys. Rev.* B **21** 1003
Krishna-murthy H R, Wilkins J W and Wilson K G 1980 *Phys. Rev.* B **21** 1044
[27] Bulla R, Tong N H and Vojta M 2003 *Phys. Rev. Lett.* **91** 170601
[28] Bulla R, Lee H J, Tong N H and Vojta M 2005 *Phys. Rev.* B **71** 045122
[29] Anders F B and Schiller A 2005 *Phys. Rev. Lett.* **95** 196801
[30] Costi T A 1997 *Phys. Rev.* B **55** 3003
[31] Bulla R, Costi T A and Vollhardt A 2001 *Phys. Rev.* B **64** 045103